Investigation of Electron Transfer through the Interfacial Electrical Double Layers of Various Micelles

Masamichi FUJIHIRA,* Masahiro YANAGISAWA, and Toshihiro KONDO#
Department of Biomolecular Engineering, Tokyo Institute of Technology, 4259, Nagatsuta, Midori-ku, Yokohama 227
(Received June 4, 1993)

In order to estimate the inner potential difference of an electrical double layer (EDL) created between the ionic hydrophilic head group of the amphiphile and its counter ion, the electrochemical characteristics of the ferrocene derivatives solubilized in three kinds of micelles were measured, and are discussed so as to clarify the effect of the EDL on the electron transfer through the interface.

Studies of photoinduced electron transfer have been of great significance in many areas of physics, chemistry, and biology. Photoinduced electron transfers involving organic assemblies have been extensively studied during the last two decades in connection with artificial photosynthesis and molecular devices.[1—8] We have investigated photoinduced electron transfer kinetics in heterogeneous A/S[9,10] or D/S[10,11] Langmuir–Blodgett (LB) films. Especially, the dependence of the photoinduced electron transfer rate on the standard free-energy difference of the reaction, i.e. the energy gap (ΔG°)[10] was studied in detail. Then, the effect of the inner potential difference in the electrical double layer (EDL) created between the ionic hydrophilic head group of the amphiphile and its counter ion was suggested.[11]

Ionic micelles have a similar EDL on the surface, and photoinduced electron transfer through the surface EDL of micelles has also been studied.[12] In this paper, the electrochemical characteristics of ferrocene derivatives solubilized and immobilized in an anionic, a cationic, and a nonionic micelles are described and discussed in order to clarify the effect of the EDL on electron transfer through the interface.

Experimental

1. Materials. Hexanoylferrocene and hexylferrocene were synthesized by conventional methods. Butylferrocene (Tokyo Kasei Kogyo) was purified by column chromatography on silica gel with hexane. Dodecyltrimethylammonium bromide (DTAB, Tokyo Kasei Kogyo) was recrystallized once by methanol. Poly[oxyethylene(10)] octylphenyl ether (TX-100, Wako Pure Chemical Industries), sodium dodecyl sulfate (SDS, Wako Pure Chemical Industries, biochemical grade), and ammonium chloride (Merck, Suprapur) were used as received. The molecular structures as the surfactants and ferrocene derivatives are shown in Fig. 1.

2. Electrochemical and Surface Potential Measurements. The solutions for electrochemical measurements were prepared as follows. After one milliliter of 0.25 M chloroform solution (1 M=1 mol dm^{-3}) of ferrocene derivative was poured into a 300 ml Schlenk vessel, chloroform was removed in vacuo. Surfactant (0.025 mol) and ammonium chloride as the supporting electrolyte were added, and the atmosphere in the Schlenk vessel was replaced by nitrogen. Pure water (250 ml) from a Milli-Q system (Millipore) bubbled by nitrogen was added into the Schlenk vessel and stirred for 3 d.

Voltammetry with a rotating glassy carbon (GC) disk electrode with a rotator (Nikko Keisoku, RRDE-1) and cyclic voltammetry with a GC disk electrode were carried out with a conventional potentiostat (Nikko Keisoku, NPGFZ-2501-A). A saturated calomel electrode (SCE), a GC rod, and the GC rotating or the GC disk electrode were used as the reference electrode, the counter electrode, and the working electrode, respectively.

The surface potential of an aqueous 0.1 M surfactant solution at the air–water interface was measured by a surface potential meter (Kyowa Interface Science, SEP). All of the measurements were carried out at room temperature (ca. 20 °C).

Results and Discussion

Curves (a), (b), and (c) in Fig. 2 show voltammograms on a rotating GC disk electrode of 1 mM butylferrocene solubilized in 0.1 M NH_4Cl aqueous solutions containing a 0.1 M surfactant of DTAB, TX-100, and SDS, respectively. It is clear from a comparison of these voltammograms that the half-wave potential ($E_{1/2}$) of butylferrocene solubilized by SDS was shifted to a potential ca. 0.1 V more negative than those by DTAB

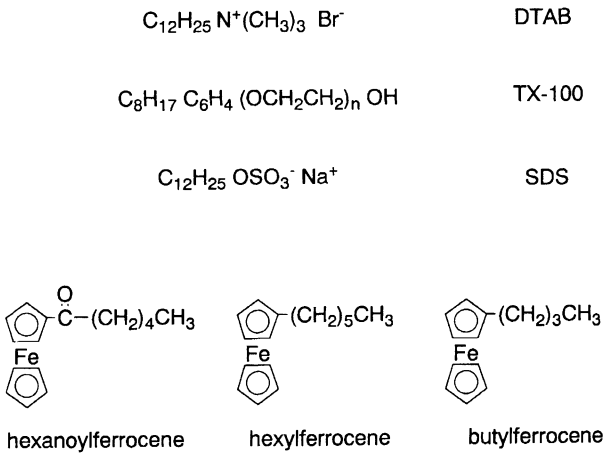

Fig. 1. Structures of dodecyltrimethylammonium bromide (DTAB), poly[oxyethylene(10)] octylphenyl, ether (TX-100), sodium dodecyl sulfate (SDS), hexanoylferrocene, hexylferrocene, and butylferrocene.

#Present address: Department of Chemistry, Faculty of Science, Hokkaido University, Sapporo 060.

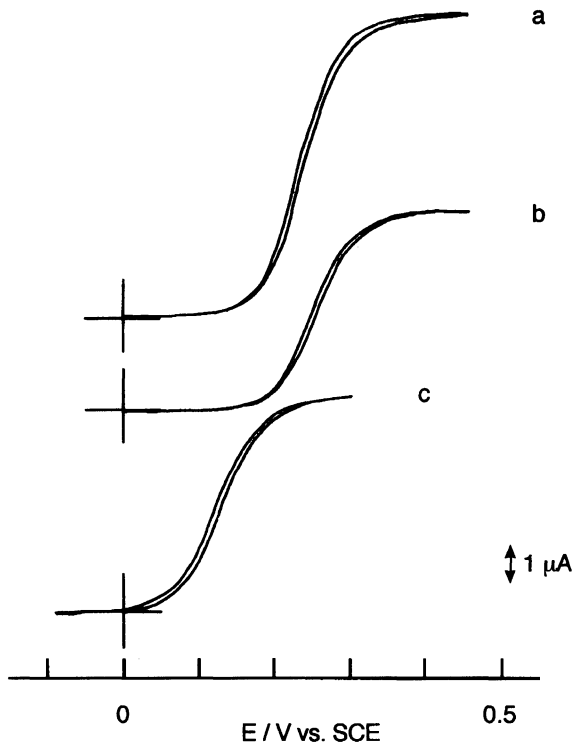

Fig. 2. Voltammograms on the rotating GC disk electrode of 1 mM butylferrocene in 0.1 M NH_4Cl containing 0.1 M surfactant. Scan rate, 4 mV s^{-1}; ω, 1600 rpm. (a) DTAB; (b) TX-100; (c) SDS.

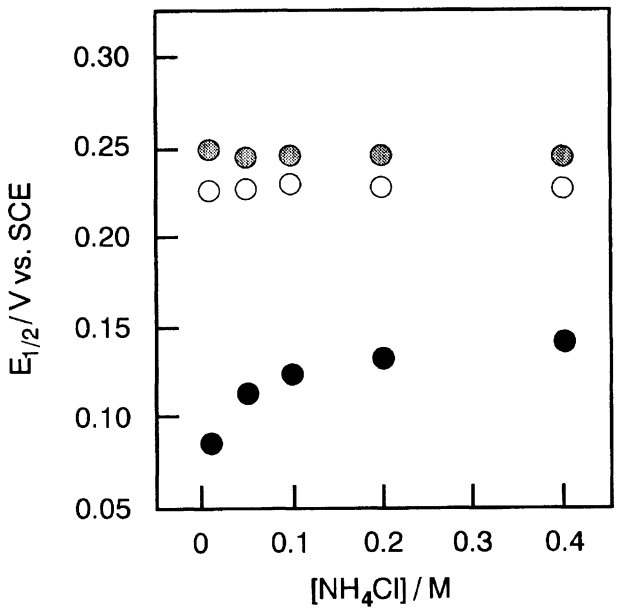

Fig. 3. Plots of $E_{1/2}$ vs. [NH_4Cl] of butylferrocene in a micellar solution: DTAB (○); TX-100 (○); SDS (●).

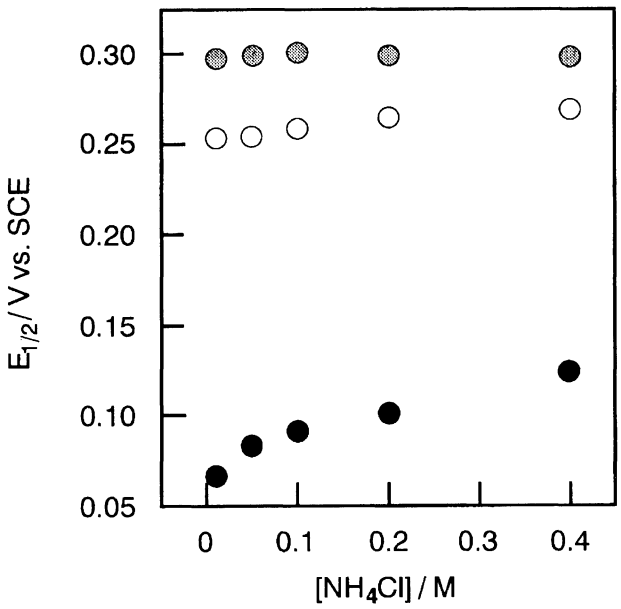

Fig. 4. Plots of $E_{1/2}$ vs. [NH_4Cl] of hexylferrocene in a micellar solution: DTAB (○); TX-100 (○); SDS (●).

and TX-100. Although $E_{1/2}$ in the DTAB system was slightly more negative than that in TX-100, their difference was negligible compared with those between SDS and DTAB, or TX-100.

When these values of $E_{1/2}$ for these three solubilized systems were plotted as a function of the concentration of NH_4Cl added as the supporting electrolyte, the curves shown in Fig. 3 were obtained. Although the values of $E_{1/2}$ for the SDS system decreased with decreasing the supporting electrolyte concentration, almost no dependence of $E_{1/2}$ on the concentration of NH_4Cl was observed for the DTAB and TX-100 systems. A similar dependence was also observed for solubilized hexylferrocene and hexanoylferrocene, as shown in Figs. 4 and 5, respectively.

The changes in the surface potentials (E) of 0.1 M surfactant aqueous solutions as a function of the NH_4Cl concentrations are also shown in Fig. 6. Along with a decrease in the NH_4Cl concentration, the E for the SDS system was shifted to the cathodic direction, while that for the DTAB system shifted to the anodic direction. However, as can be seen from Fig. 6, almost no change in E was observed for the TX-100 system.

The experimental findings indicate that the potential difference ($\Delta\phi$) due to the EDL created between the ionic head groups and the counter ions in solution varied and decreased down to $\Delta\phi$ of the compact EDL along with an increase in the NH_4Cl concentration, and contributed linearly to the measured surface potentials. Contrary, no change was observed for the TX-100, which is reasonable, since in this system a free charge is absent on the hydrophilic head group of TX-100 and there is no diffused EDL; thus, the EDL created only by the aligned dipole moments was only little affected by the change in the concentration of the supporting electrolyte. i) The difference in the surfactant surface densities (Γ) in the monolayers at the air-water interfaces of these surfactant solutions and, the there-

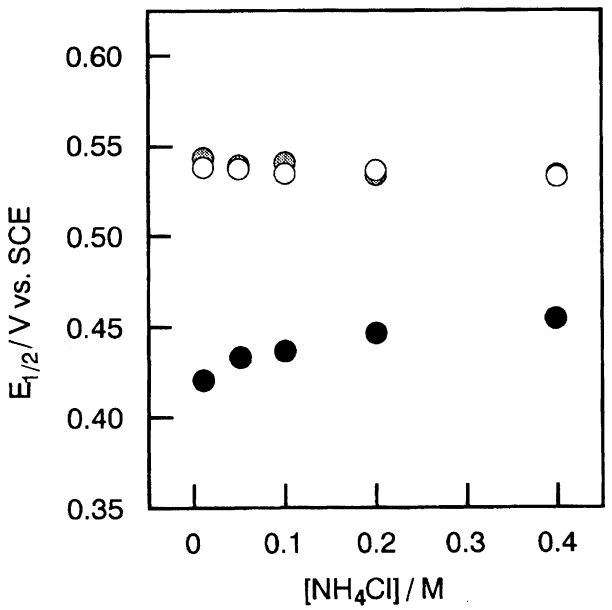

Fig. 5. Plots of $E_{1/2}$ vs. [NH_4Cl] of hexanoylferrocene in a micellar solution: DTAB (○); TX-100 (○); SDS (●).

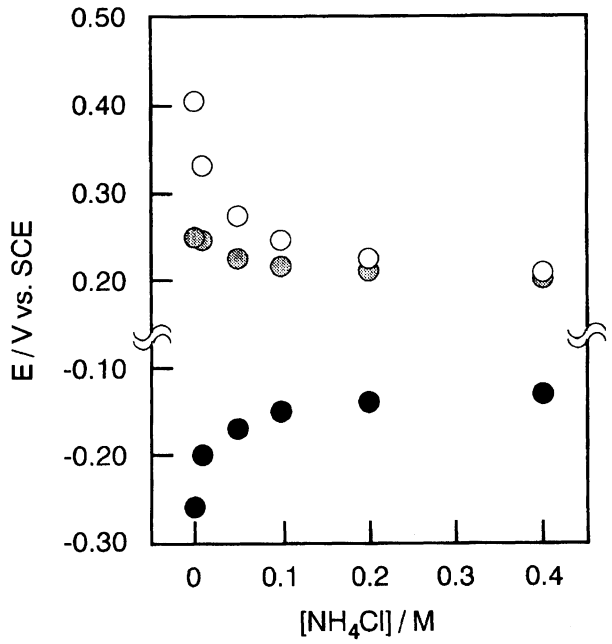

Fig. 6. Plots of the surface potentials vs. [HN_4Cl] of the monolayer at the air/water interface for 0.1 M aqueous surfactant solutions: DTAB (○); TX-100 (○); SDS (●).

fore, the difference in the Γ of the surface dipole due to the hydrophobic tail end of $-CH_3$ and ii) the difference in the dipole moments due to the compact EDL of the ionic or nonionic head groups and their density Γ may account for the difference in the surface potentials at high NH_4Cl concentrations.

From a comparison of Figs. 3 and 6, it is clear that there is an effect of the micellar surface EDL on $E_{1/2}$ of solubilized butylferrocene for the SDS system, but not the DTAB system. In the case of the TX-100 system, this effect is not so obvious, since the surface potential, itself, was independent of the NH_4Cl concentration.

The different electrochemical behavior among three solubilized systems can be interpreted in terms of the difference in the solubilization of the electrochemical product, i.e. a ferrocenium (Fc^+) cation, as schematically illustrated in Fig. 7. Namely, for SDS, since the product is also solubilized after the electrochemical oxidation, there is the effect of the EDL on the electrochemical potential of Fc^+, and thus $E_{1/2}$, which differ from those of the reference standard state in the aqueous phase, i.e. outside of the micelle. In contrast, for DTAB, Fc^+ cannot be solubilized in the cationic micelle due to the electrostatic repulsion between Fc^+ and the cationic surface charge of the DTAB micelle, and also its hydrophilicity. Consequently, the initial and the final states of the electrochemical process

$$Fc_{\text{in micelle}} \rightarrow Fc^+_{\text{in water}} + e_{\text{in electrode}} \quad (1)$$

are not appreciably affected by the change in the NH_4Cl concentration. For TX-100, since there was no appreciable change in the surface potential, we cannot conclude from only this $E_{1/2}$ measurement whether Fc^+ is solubilized in the poly(oxyethylene) layer surrounding the micellar surface or in the water phase, as illustrated in Fig. 7(c). To determine the location of the solubilization site of Fc^+ in the TX-100 micellar solution, further observations, such as absorption spectroscopy, are still necessary.

Figure 8 shows the dependence of $E_{1/2}$ determined from cyclic voltammetry of 1 mM butylferrocene in 0.1 M SDS upon the NH_4Cl concentration. Almost the same tendency can be seen as that observed by voltammetry on the rotating GC disk electrode shown in Fig. 3.

In the following, how the extent of $\Delta\phi$ contributes to the change in $E_{1/2}$ for SDS is discussed by referring to the literature. When we discuss the redox potential of Fc/Fc^+ in a solubilized system, it is necessary to take into account the solubilization equilibrium of the reduced and oxidized form of Fc between the micellar and the water phases[13] shown in Fig. 9. As described above, for SDS, since both Fc and Fc^+ are located inside the micellar phase, an electron passes through the EDL during the oxidation of one Fc, but Fc^+ does not. In this case, the solvation energy change of Fc^+ due to the difference in the dielectric constants between the micellar and the water phase and the potential difference ($\Delta\phi$) at the surface EDL of the micelle must be taken into account as follows:

$$E_{1/2}{}^{\mathrm{r}} = E_{1/2,\mathrm{w}}{}^{\mathrm{r}} + \mathrm{e}(1/\varepsilon_{\mathrm{m}} - 1/\varepsilon_{\mathrm{w}})(2z+1)/2a + \Delta\phi, \quad (2)$$

where $E_{1/2}{}^{\mathrm{r}}$ and $E_{1/2,\mathrm{w}}{}^{\mathrm{r}}$ are the half-wave potentials of the solubilized Fc/Fc^+ and Fc/Fc^+ in water, respectively, and the second term corresponds to the necessary

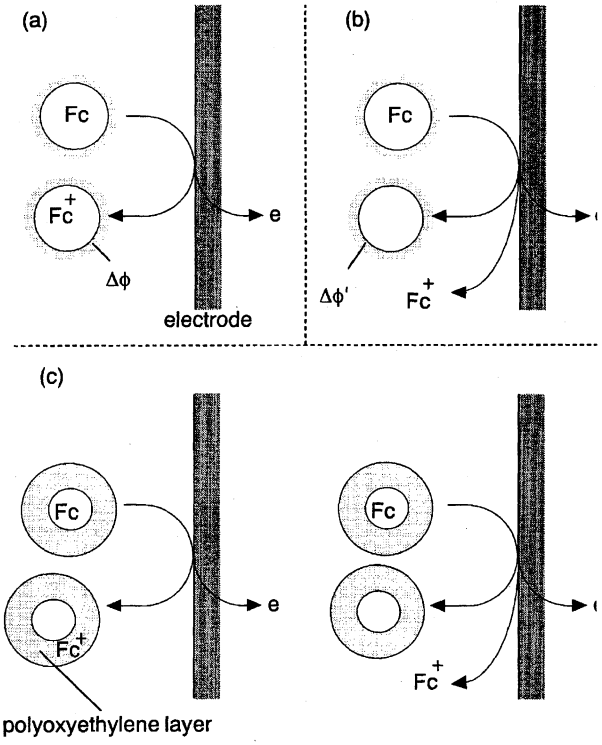

Fig. 7. Schematic view of the electrochemical oxidation of ferrocene in micelles: (a) anionic micelle; (b) cationic micelle; (c) nonionic micelle.

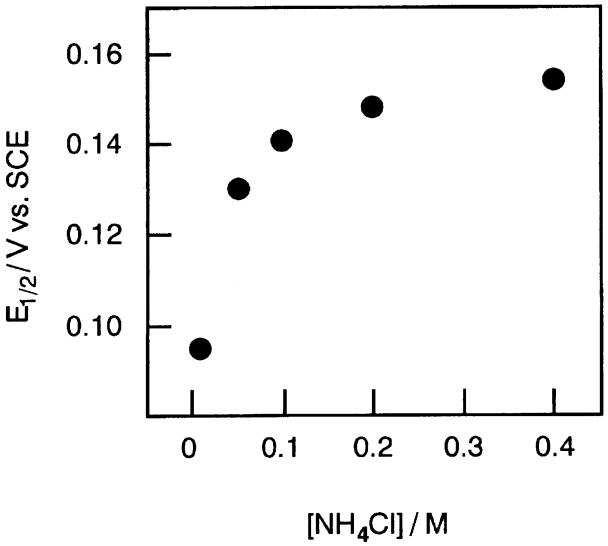

Fig. 8. Plots of $E_{1/2}$ determined from cyclic voltammetry vs. $[HN_4Cl]$ of butylferrocene in a micellar solution in 0.1 M SDS.

work for bringing Fc^+ from water to the micellar phase, calculated by the Born equation.[14]

The work for bringing an ion with a charge of ze from the vacuum to the medium with dielectric constant ε_S is given by equation (i) in Fig. 10.[14] Therefore, the energy difference in the oxidation of Fc between the micellar and the water phase based on the Born equation is given by equation (ii). This is the origin of the second term

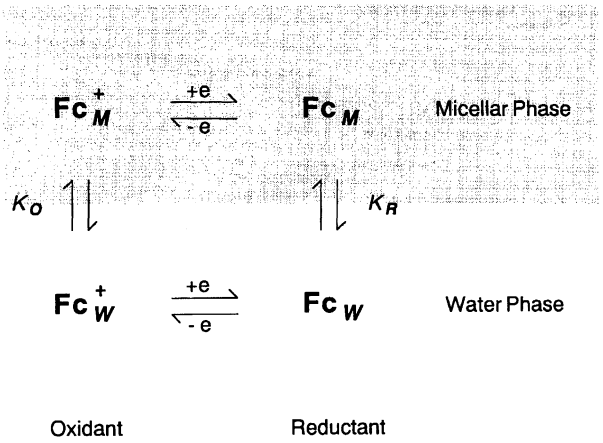

Fig. 9. Electron-transfer reaction at the ferrocene coupled with micelle-solubilization equilibria.

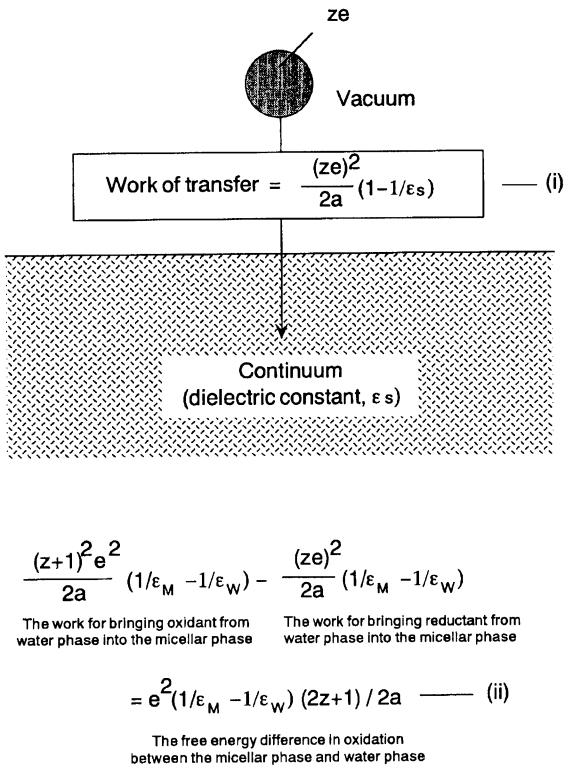

Fig. 10. Derivation of the free-energy difference in the oxidation between the micellar and water phases.

in Eq. 2.

If we subtract first term in Eq. 2 from the left-hand side of Eq. 2, we obtain

$$\Delta E_{1/2}{}^{r} = \{e(1/\varepsilon_m - 1/\varepsilon_w)/2a\}(2z+1) + \Delta\phi. \quad (3)$$

From this equation, if the $E_{1/2}$'s were measured for various redox couple with different z, and the values were plotted as a function of $2z+1$, then $e(1/\varepsilon_m - 1/\varepsilon_w)/2a$ could be obtained from the slope and $\Delta\phi$ from the intercept. An attempt to evaluate the slope was made by Ohsawa et al.,[13] as shown in Fig. 11, by using various redox couples. From these plots, the values of 9—

25 mV are obtained as the slope. On the other hand, Suga et al. has already determined $\Delta E_{1/2}{}^{r}$ for viologens solubilized in aq SDS;[15] when these values were plotted together with the value determined in the present work for butylferrocene as a function of $2z+1$, the plot shown in Fig. 12 was obtained, where 0.1 M was used as the concentration of the supporting electrolytes. The intercepts given by extrapolation of the solid lines are ca. 145 mV, while the intercepts given by the slopes by Ohsawa shown in Fig. 11 are ca. 90 mV, as shown by the dashed lines in Fig. 12. Although there is only a slight difference in the values of $\Delta\phi$ obtained from these intercepts, the values of $\Delta\phi$ were estimated to be 80—150 mV in the presence of 0.1 M of the supporting electrolytes. The shift of ca. 100 mV in $E_{1/2}$ observed for in Fig. 2 should correspond to the summation of the slope and $\Delta\phi$, since for the ferrocene derivatives z is zero. The sum of the values for the slope and $\Delta\phi$ estimated above (90—175 mV) is in fairly good agreement with the shift in $E_{1/2}$ of ca. 100 mV.

Conclusion

It was found that when ferrocene derivatives were solubilized in SDS micellar solutions, the values of $E_{1/2}$ reflect $\Delta\phi$ of the EDL at the micellar surface, which is evident from a comparison between the dependence of $E_{1/2}$ and the surface potential (E) on the supporting electrolyte concentration. On the other hand, in the DTAB micellar system, no effect of the EDL was observed. This implies that the oxidized product Fc^{+} is solubilized in the micellar phase for SDS, but comes out to the water phase for DTAB. The difference in $E_{1/2}$'s in the micellar and the water phase is expected to have two origins based on a consideration of the difference in the dielectric constant of these media; the other is the effect of the electrical potential difference ($\Delta\phi$) across the EDL. From an analysis of $\Delta E_{1/2}$ as a function of $2z+1$, the contribution from $\Delta\phi$ was estimated to be 80—150 mV, and that from the Born term to be 9—25 mV. The sum of these contributions is in good agreement with the shift in $E_{1/2}$ between SDS and DTAB or TX-100.

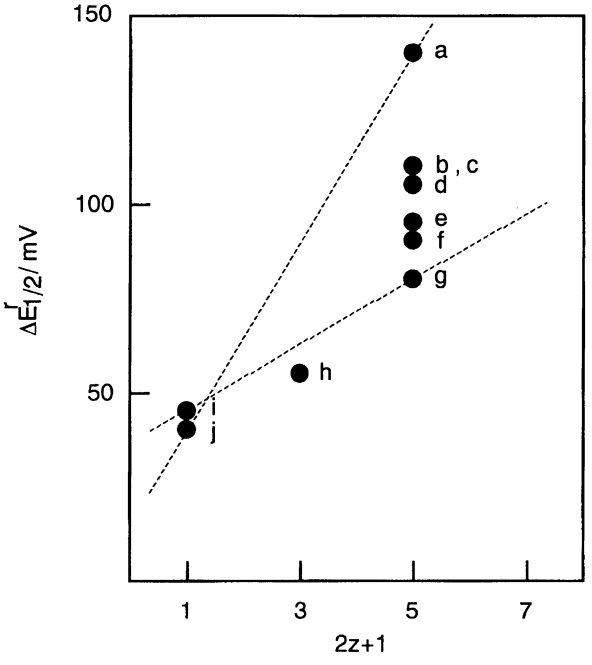

Fig. 11. Correlation between $\Delta E_{1/2}{}^{r}$ and $2z+1$. (a) $Os(4\text{-}dmbpy)_3^{3+/2+}$; (b) $Os(phen)_3^{3+/2+}$; (c) $Fe(phen)_3^{3+/2+}$; (d) $Os(5\text{-}Clphen)_3^{3+/2+}$; (e) $Os(dmbpy)_3^{3+/2+}$; (f) $Os(bpy)_3^{3+/2+}$; (g) $Fe(bpy)_3^{3+/2+}$; (h) methylviologen$^{2+/+}$; (i) $Fe(bpy)_2(CN)_2^{+/0}$; (j) $Ru(bpy)_2(CN)_2^{+/0}$. [Y. Ohsawa, Y. Shimazaki, and S. Aoyagui, *J. Electroanal. Chem.*, **114**, 235 (1980)].

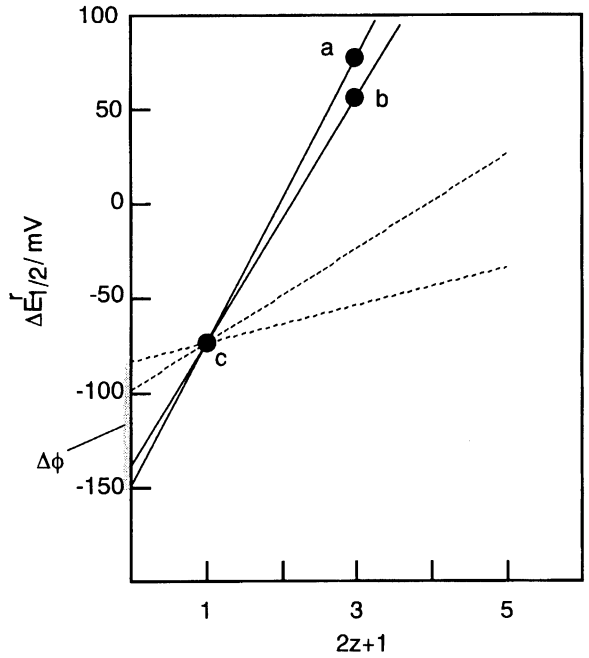

Fig. 12. Correlation between $\Delta E_{1/2}{}^{r}$ and $2z+1$. (a) ethylviologen$^{2+/+*}$; (b) methylviologen$^{2+/+*}$; (c) butylferrocene$^{+/0}$. *K. Suga and M. Fujihira, "Extended abstract of "40th ISE Meeting," at Kyoto, 1988, Vol 2, p. 976.

References

1) H. Kuhn, *J. Photochem.*, **10**, 111 (1979).
2) D. Möbius, *Acc. Chem. Res.*, **14**, 63 (1981).
3) H. Gerischer, *Photochem. Photobiol.*, **16**, 243 (1972).
4) N. Sutin, *J. Photochem.*, **10**, 19 (1979).
5) G. L. Gaines, Jr., P. E. Behnken, and S. J. Valenty, *J. Am. Chem. Soc.*, **100**, 6549 (1978).
6) K. Kemmitz, N. Tamai, I. Yamazaki, N. Nakashima, and K. Yoshihara, *J. Phys. Chem.*, **90**, 5094 (1986).
7) H. Takemura, T. Saji, M. Fujihira, S. Aoyagui, K. Hashimoto, and T. Sakata, *Chem. Phys. Lett.*, **122**, 496 (1985).
8) K. Hashimoto, M. Hiramoto, T. Sakata, H. Muraki, H. Takemura, and M. Fujihira, *J. Phys. Chem.*, **91**, 6198 (1987).

9) M. Fujihira, K. Aoki, S. Inoue, H. Takemura, H. Muraki, and S. Aoyagui, *Thin Solid Films*, **132**, 221 (1985).
10) M. Fujihira, K. Nishiyama, and K. Aoki, *Thin Solid Films*, **160**, 317 (1988).
11) T. Kondo, H. Yamada, K. Nishiyama, K. Suga, and M. Fujihira, *Thin Solid Films*, **179**, 463 (1989).
12) D. Grand and S. Hautecloque, *J. Phys. Chem.*, **94**, 837 (1990).
13) Y. Ohsawa, Y. Shimazaki, and S. Aoyagui, *J. Electroanal. Chem.*, **114**, 235 (1980).
14) J. O'M. Bockris and A. K. N. Reddy, "Modern Electrochemistry," Plenum Press, New York (1970), Vol. 1, p. 56.
15) K. Suga and M. Fujihira, "Extended Abstracts of 40th ISE Meeting," at Kyoto, 1988, Vol. 2, p. 976.